ANEXO A. Norma ASTM D3663-03. Determinación de Área Superficial.

Designation: D3663 – 03 (Reapproved 2008)

Standard Test Method for Surface Area of Catalysts and Catalyst Carriers[1]

This standard is issued under the fixed designation D3663; the number immediately following the designation indicates the year of original adoption or, in the case of revision, the year of last revision. A number in parentheses indicates the year of last reapproval. A superscript epsilon (ε) indicates an editorial change since the last revision or reapproval.

1. Scope

1.1 This test method covers the determination of surface areas of catalyst and catalyst carriers that have Type II or IV nitrogen adsorption isotherms, and at least 1 m^2/g of area. A volumetric measuring system is used to obtain at least four data points which fit on the linear BET[2] line.

1.2 The values stated in SI units are to be regarded as the standard. The values given in parentheses are for information only.

1.3 *This standard does not purport to address all of the safety concerns, if any, associated with its use. It is the responsibility of the user of this standard to establish appropriate safety and health practices and determine the applicability of regulatory limitations prior to use.*

2. Referenced Documents

2.1 *ASTM Standards:*[3]

D3766 Terminology Relating to Catalysts and Catalysis

E177 Practice for Use of the Terms Precision and Bias in ASTM Test Methods

E456 Terminology Relating to Quality and Statistics

E691 Practice for Conducting an Interlaboratory Study to Determine the Precision of a Test Method

3. Terminology

3.1 Consult Terminology D3766 for definitions of other terms used.

3.2 *Definitions:*

3.2.1 *surface area of a catalyst*—the total surface of the catalyst. It is expressed in square metres per gram.

3.3 *Symbols:*

P_{H_1} = initial helium pressure, torr
P_{H_2} = helium pressure after equilibration, torr
T_{H_1} = temperature of manifold at initial helium pressure, °C
T_{H_2} = temperature of manifold after equilibration, °C
P_1 = initial N_2 pressure, torr
T_1 = manifold temperature at initial N_2 pressure, K
T_1' = manifold temperature at initial N_2 pressure, °C
P_2 = pressure after equilibration, torr
P_0 = liquid nitrogen vapor pressure, torr
T_s = liquid nitrogen temperature, K
X = relative pressure, P_2/P_0
V_d = volume of manifold, cm^3
V_x = extra volume bulb, cm^3
V_s = dead-space volume, cm^3
W_s = mass of sample, g
W_1 = tare mass of sample tube, g
W_2 = sample + tare mass of tube, g
V_{ds} = volume of nitrogen in the dead-space, cm^3
V_1 = see 10.4.4
V_2 = see 10.4.6
V_t = see 10.4.7
V_a = see 10.4.9
V_m = see 10.8
T_{1x} = initial extra-volume bulb temperature, K
$T_{1x}'(i)$ = initial extra-volume bulb temperature, °C
T_{2x} = extra-volume bulb temperature after equilibrium, K
$T_{2x}'(i)$ = extra-volume bulb temperature after equilibrium, °C

4. Summary of Test Method

4.1 The surface area of a catalyst or catalyst carrier is determined by measuring the volume of nitrogen gas adsorbed at various low-pressure levels by the catalyst sample. Pressure differentials caused by introducing the catalyst surface area to a fixed volume of nitrogen in the test apparatus are measured and used to calculate BET surface area.

5. Apparatus [4]

5.1 A schematic diagram of the apparatus is shown in Fig. 1. It may be constructed of glass or of metal. It has the following features:

[1] This test method is under the jurisdiction of ASTM Committee D32 on Catalysts and is the direct responsibility of Subcommittee D32.01 on Physical-Chemical Properties.

Current edition approved April 1, 2008. Published April 2008. Originally approved in 1978. Last previous edition approved in 2003 as D3663–03. DOI: 10.1520/D3663-03R08.

[2] Brunauer, Emmett, Teller, *Journal of American Chemical Society*, JACS, No. 60, 1938, p. 309.

[3] For referenced ASTM standards, visit the ASTM website, www.astm.org, or contact ASTM Customer Service at service@astm.org. For *Annual Book of ASTM Standards* volume information, refer to the standard's Document Summary page on the ASTM website.

[4] Automated equipment is commercially available.

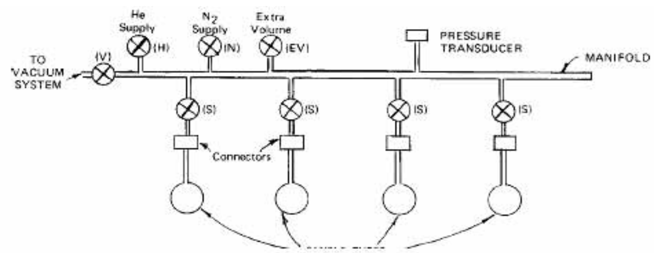

FIG. 1 Schematic Diagram of Surface Area Apparatus

5.1.1 *Distribution Manifold*, having a volume between 20 and 35 cm^3, (V_d), known to the nearest 0.05 cm^3. This volume is defined as the volume between the stopcocks or valves and includes the pressure gage.

5.1.2 *Vacuum System*, capable of attaining pressures below 10^{-4} torr (1 torr = 133.3 Pa). This will include a vacuum gage (not shown in Fig. 1). Access to the distribution manifold is through the valve *V*.

5.1.3 *Constant-Volume Gage or Mercury Manometer*, capable of measurements to the nearest 0.1 torr, in the range from 0 to 1000 torr (1 torr = 133.3 Pa).

NOTE 1—See, for example, the article by Joy[5] for a description of a constant-volume manometer.

5.1.4 *Valve (H)*, from the helium supply to the distribution manifold.

5.1.5 *Valve (N)*, from the nitrogen supply to the distribution manifold.

5.1.6 The connection between the sample tube and the *S* valve can be a standard-taper glass joint, a glass-to-glass seal, or a compression fitting.

5.1.7 *Extra Volume Bulb*, (V_x), should be 100 to 150 cm^3, known to the nearest 0.05 cm^3. V_x includes the volume of the stopcock bore in the glass apparatus.

5.2 *Sample Tubes*, with volumes from 5 to 100 cm^3 depending on the application. Markings should be placed on the sample tubes about 30 to 50 mm below the connectors to indicate the desired liquid nitrogen level.

5.3 *Heating Mantles or Small Furnaces*.

5.4 *Dewar Flasks*.

5.5 *Laboratory Balance*, with 0.1-mg (10^{-7}-kg) sensitivity.

5.6 *Thermometer or Thermocouple*, for measuring the temperature of the distribution manifold [$T_1'(i)$ or $T_2'(i)$] in degrees Celsius.

5.6.1 It is preferred that the manifold be thermostated at a particular temperature, a few degrees above ambient, to obviate the necessity of recording this temperature at each reading.

5.7 *Thermometer*, for measuring the temperature of the liquid nitrogen bath [$T_s(i)$] in kelvins. This will preferably be a nitrogen vapor-pressure thermometer, often referred to in a commercial instrument as a pressure saturation tube, from which P_0 values may be derived.

[5] Joy, A. S., *Vacuum*, Vol 3, 1953, p. 254.

6. Reagents

6.1 *Purity of Reagents*—Reagent grade chemicals shall be used in all tests. Unless otherwise indicated, it is intended that all reagents shall conform to the specifications of the Committee on Analytical Reagents of the American Chemical Society, where such specifications are available.[6] Other grades may be used, provided it is first ascertained that the reagent is of sufficiently high purity to permit its use without lessening the accuracy of the determination.

6.2 *Helium Gas*—A cylinder of helium gas at least 99.9 % pure.

6.3 *Liquid Nitrogen*, of such purity that P_0 is not more than 20 torr above barometric pressure. A fresh daily supply is recommended.

6.4 *Nitrogen Gas*—A cylinder of nitrogen gas at least 99.999 % pure.

7. Procedure—Sample Preparation and Degassing

7.1 Select a sample tube of the desired size. A 5-cm^3 sample tube is preferred for samples not exceeding about 1 g, to minimize the dead-space. However, a 25-cm^3 sample tube may be preferred for finely powdered catalysts, to avoid "boiling" when degassing is started.

7.2 Fill the sample tube with nitrogen or helium, at atmospheric pressure, after removing air by evacuation. This may be done on the surface area unit, or on a separate piece of equipment.

7.3 Remove the sample tube from the system, cap, and weigh. Record the mass as W_1.

7.4 Place the catalyst sample, whose mass is known approximately, into the sample tube. Choose the sample size to provide an estimated total sample surface area of 20 to 100 m^2.

7.5 Attach the sample tube to the apparatus. If other samples are to be run, attach them at this time to the other ports.

7.6 Open the *S* valves where there are samples.

7.7 It may be necessary to close the *V* valve system periodically to protect the diffusion pump fluid from exposure to pressures above 0.1 torr for periods of more than 30 s. Close the valve off for 2 min.

[6] *Reagent Chemicals, American Chemical Society Specifications*, American Chemical Society, Washington, DC. For Suggestions on the testing of reagents not listed by the American Chemical Society, see *Annual Standards for Laboratory Chemicals*, BDH Ltd., Poole, Dorset, U.K., and the *United States Pharmacopeia and National Formulary*, U.S. Pharmacopeial Convention, Inc. (USPC), Rockville, MD.

7.8 Install a heating mantle or furnace around each sample and raise the temperature to about 300°C (573 K).

NOTE 2—Take special precautions if the moisture content exceeds approximately 5 % to avoid "bumping" of powdered catalyst, and to avoid surface area loss by self-steaming. It is recommended that the heating rate not exceed 100 K/h under these circumstances.

7.9 Continue degassing at about 300°C (573 K) for a minimum of 3 h, at a pressure not to exceed 10^{-3} torr. Overnight degassing is permissible.

NOTE 3—Certain materials will decompose at 300°C (for example, alumina hydrates) or will sinter (for example, platinum black). Lower degassing temperatures are permissible for such materials; however, the degassing temperature should be specified when reporting the results.

7.10 Remove the heating mantles, and allow the samples to cool.

7.11 Close the *EV* valve, if open.

7.12 Close the *S* valve.

7.13 It is permissible to exercise the option of preliminary degassing on an external unit. In such a case, follow the procedures of 7.4-7.11 and then repeat on the surface area unit, except that the degassing time in 7.9 should not exceed 1 h.

7.14 If it is desired to weigh the sample after preliminary degassing on an external unit, backfill with the same gas used in 7.2 to above atmospheric pressure. Close the *S* valve.

7.15 Detach the sample tube from the apparatus, recap with the stopper used previously, and weigh. Record the mass as W_2.

7.16 Remove the backfilled gas by evacuation to less than 10^{-4} torr at room temperature.

8. Procedure—Dead-Space Determination

8.1 From this point on, each sample being tested for surface area must be run on an individual basis. Thus each Step 8.2-9.17 must be carried out separately for each tube in test.

8.2 The "dead-space" is the void volume of the charged sample tube, including the *S* valve, when the tube is immersed in liquid nitrogen to the proper depth (see 5.2).

NOTE 4—The dead-space may be determined after the nitrogen adsorption, if more convenient, as long as adequate degassing precedes it. In that case, replace the liquid nitrogen bath after Step 9.14 before proceeding with Steps 8.3-8.9.

8.3 Place a Dewar flask of liquid nitrogen around the sample and adjust the liquid level to a fixed point on the sample tube. Maintain this level throughout the test.

8.4 Zero the pressure gage.

8.5 Admit the helium gas into the manifold to a pressure of 600 to 900 torr by carefully opening the *H* valve. Record this pressure as P_{H1}, and the manifold temperature, T_{H1}.

8.6 Open the *S* valve to admit helium to the sample.

8.7 After about 5 min of equilibration, readjust the liquid nitrogen level, and record the pressure as P_{H2}, and manifold temperature as T_{H2}.

8.8 Repeat 8.5-8.7 for each sample on the manifold.

8.9 Open all *S* valves; then slowly open the *V* valve to remove the helium gas.

8.10 When a pressure less than 0.01 torr has been attained, close the *S* valve. This operation should take 5 to 10 min.

9. Procedure—Nitrogen Adsorption

9.1 Close the *V* valve and open the *EV*valve if the extra-volume bulb is to be used, when the surface area is known to be high.

9.2 Recheck the zero setting of the pressure gage.

9.3 Admit nitrogen gas, and record the pressure as $P_1(1)$ (torr) and the temperature as $T_1'(1)$ (degrees Celsius) and read the temperature of the extra-volume bulb and record it as $T_{1x}(1)$. It is desirable, but not necessary, to choose $P_1(1)$ such that the first equilibrium adsorption pressure, $P_2(1)$, will be about 40 torr equivalent to $P_2(1)/P_0(1)$ of about 0.05. If the surface area is small, it may be desirable to eliminate use of the extra-volume bulb by closing the *EV* valve.

9.4 Open the *S* valve to admit nitrogen to the catalyst.

9.5 Allow sufficient time for equilibration, readjusting the liquid nitrogen level when necessary. Equilibrium shall be considered as attained when the pressure change is no more than 0.02 torr/min.

9.6 Record the equilibrium pressure as $P_2(1)$, manifold temperature $T_2'(1)$, and the extra volume bulb temperature $T_{2x}(1)$.

9.7 Record the liquid nitrogen temperature $[T_s(1)]$ or the nitrogen vapor pressure $[P_0(1)]$.

9.8 Close the *S* valve and close the *EV* valve; then admit nitrogen gas to increase the pressure by 100 to 200 torr, depending upon surface area. Record the pressure as $P_1(2)$, the manifold temperature as $T_1'(2)$, and the extra-volume bulb temperature as $T_{1x}'(2)$.

9.9 Open the *S* valve to admit the new increment of nitrogen to the catalyst.

9.10 Allow sufficient time for equilibration, readjusting the liquid nitrogen level as necessary. The criterion for equilibrium is defined in 9.5.

9.11 Record the equilibrium pressure as $P_2(2)$, and record $T_2'(2)$ and $T_{2x}'(2)$.

9.12 Again record $T_s(2)$ or $P_0(2)$.

9.13 Repeat Steps 9.8-9.12 until there are at least four points in the linear BET range. This will normally be from $P/P_o = 0.04$ to 0.20 or 0.25. Designate the pressures as $P_1(i)$ and $P_2(i)$, manifold temperature as $T'(i)$, and the extra-volume temperatures as $T_{1x}(i)$ and $T_{2x}(i)$. ($i = 3$ to n, where n is total number of points.)

9.14 Slowly open the *V* valve, remove the Dewar flask, and allow the sample flask to come to room temperature.

9.15 When frost has disappeared from the sample tube, wipe it dry.

9.16 Backfill the sample tube with the same gas used in 7.2 to about atmospheric pressure. Close the *S* valve.

9.17 Detach the sample tube from the apparatus, recap with the stopper used previously, and weigh. Record the mass as W_2.

10. Calculations

10.1 Calculate the mass of sample W_s, as follows:

$$W_s = W_2 - W_1 \tag{1}$$

10.2 Calculate the dead-space, V_s as follows:

$$V_s = \left(\frac{T_s V_d}{P_{H_2}}\right)\left(\frac{P_{H_1}}{(T_{H_1} + 273.2)} - \frac{P_{H_2}}{(T_{H_2} + 273.2)}\right) \tag{2}$$

NOTE 5—The user should consult IUPAC[7] for the latest value of absolute zero to use in these calculations, as 273.2 was current for this revision.

10.3 For each point, $i = 1, 2 \ldots n$, the following measurements will have been recorded:

10.3.1 For pressures $P_1(i)$ and $P_2(i)$, see 5.1.3, 9.3, 9.6, 9.8, 9.11, and 9.13.

10.3.2 For vapor pressures $P_o(i)$, or liquid nitrogen temperatures, $T_s(i)$, see 5.7, 9.7, and 9.12.

10.3.2.1 If $P_o(i)$ is not measured directly, the values of $T_s(i)$ can be converted to $P_0(i)$ by the following equation for $76 \leq T_s(i) \leq 80$:

$$P_0(i) = -107293 + 4269.71[Ts(i)] - 57.3616[Ts(i)]^2 + 0.261431[T_s(i)]^3 \tag{3}$$

10.3.3 For manifold temperatures $T_1'(i)$ and $T_2'(i)$, see 5.6, 9.3, 9.6, 9.8, 9.11, and 9.13.

10.3.4 Determine whether valve EV is open. If not, $V_x = 0$, see 5.1.7.

10.3.5 For extra-volume bulb temperatures $T_{1x}'(i)$ and $T_{2x}'(i)$; see 9.3, 9.6, 9.8, and 9.11.

10.4 For each point, $i = 1, 2 \ldots n$, calculate the following:

10.4.1 $X(i)$ = relative pressure = $P_2(i)/P_o(i)$

10.4.2 Manifold and extra-volume bulb temperatures in kelvins:

$$T_1(i) = T_1'(i) + 273.2 \tag{4}$$

$$T_2(i) = T_2'(i) + 273.2$$

$$T_{1x}(i) = T_{1x}'(i) + 273.2$$

$$T_{2x}(i) = T_{2x}'(i) + 273.2$$

10.4.3 Extra-volume bulb volume at manifold temperature $T_1(i)$:

$$V_{1x} = T_1(i) \times V_x/T_{1x}(i) \tag{5}$$

10.4.4 Volume of N_2 in manifold + extra volume, S valve, closed to catalyst (cm³ STP):

$$V_1(i) = (V_d + V_x)\left(\frac{P_1(i)}{T_1(i)}\right)\left(\frac{273.2}{760}\right) \tag{6}$$

10.4.5 Extra-Volume bulb volume at manifold temperature $T_2(i)$:

$$V_{2x} = T_2(i) \times V_x/T_{2x}(i) \tag{7}$$

10.4.6 Volume of N_2 in manifold + extra volume, S valve, open to catalyst (cm³ STP):

$$V_2(i) = (V_d + V_x)\left(\frac{P_2(i)}{T_2(i)}\right)\left(\frac{273.2}{760}\right) \tag{8}$$

See 5.1.1 and 5.1.7 for V_d and V_x.

10.4.7 Total inventory of nitrogen in the system (cm³ STP):

$$V_t(i) = V_t(i-1) + V_1(i) - V_2(i-1) \tag{9}$$

$$V_t(0) = 0$$

$$V_2(0) = 0$$

10.4.8 Volume of nitrogen in the dead-space (cm³ STP):

[7] IUPAC Secretariat, PO Box 13757, Research Triangle Park, NC 27709-3757.

$$V_{ds}(i) = \left(\frac{273.2\ V_s \times P_2(i)}{760 T_s}\right)\left(1 + \frac{0.05\ P_2(i)}{760}\right) \tag{10}$$

See 10.2 for V_s.

10.4.8.1 The deviation from the ideal gas law of nitrogen at liquid nitrogen temperature is 5 % at one atmosphere, proportional to pressure. Although the non-ideality constant should be applied *only* to the volume of nitrogen within the section of the sample cell that is immersed in the liquid nitrogen, the added complexity to the experimental procedure needed to determine the fraction of the volume at liquid nitrogen temperature is not justified by the increased accuracy.

10.4.9 The quantity of gas adsorbed (cm³ STP/g):

$$V_a(i) = \frac{V_t(i) - V_2(i) - V_{ds}(i)}{W_s} \tag{11}$$

See 10.1 for W_s.

10.4.10 The BET function, when $X(i) \geq 0.04$:

$$BET(i) = \left(\frac{X(i)}{V_a(i)}\right)\left(\frac{1}{[1 - X(i)]}\right) \tag{12}$$

10.5 Construct the BET plot, by plotting $X(i)$ as the abscissa, BET(i) as the ordinates.

10.6 Using a straightedge, draw a line through the linear region. Deviations from the straight line, if any, should be below the line at low $X(i)$, above the line at high $X(i)$, but not apparent within the linear region.

10.7 Determine the slope (S) and intercept (I) of the straight line.

10.7.1 This is preferably done by a least squares calculation, choosing only those points which fall on the straight line. If a point in the linear region is not on the straight line, discard the run. It will generally be clear by inspection of the BET plot which points to choose to define the straight line. When the proper choice has been made, deviations of individual points from the straight line should not exceed about 0.6 % of the value of the ordinate. A deviation as large as 1 % is excessive.

10.8 Calculate V_m, the volume of adsorbate required to complete one statistical monolayer (cm³ STP/g)

$$V_m = 1/(S + I) \tag{13}$$

10.9 Surface area = 4.353 × V_m. This assumes a value of 16.2 Å² (1 Å = 0.1 nm) for the cross-sectional area of a nitrogen molecule.

11. Report

11.1 Report the surface area to three significant figures.

11.2 The report shall include pretreatment, and outgassing temperatures.

12. Precision and Bias [8]

12.1 *Test Program*—An interlaboratory study was conducted in which the surface area was measured on three different materials in seven different laboratories on nine different instruments. Each laboratory performed three replicate analysis on each of the samples over a period of time. All samples were degassed at 300°C under vacuum and evaluated

[8] Supporting data have been filed at ASTM International Headquarters and may be obtained by requesting Research Report D32-1031.

Practice E691 was followed for the analysis of the data. Analysis details are in the research report.

12.2 *Precision*—Pairs of tests results obtained by a procedure similar to that described in the study are expected to differ in absolute value by less than 2.772 S, where 2.772 S is the 95% probability limit on the difference between two test results, and S is the appropriate estimate of standard deviation. Definitions and usage are given in Terminology E456 and Practice E177, respectively.

Sample	(consensus mean) m²/g	Interval m²/g (%)	95% Reproducibility Interval m²(%)
RM8570	10.7	1.1 (10.4)	2.5 (23.0)
RM8571	160	8.9 (5.6)	9.8 (6.1)
RM8572	289	7.0 (2.4)	11.9 (4.1)

12.3 *Bias*—This test method is without known bias.

13. Keywords

13.1 catalyst; nitrogen adsorption; surface area

ANEXO B. Norma ASTM D3663-03. Distribución de Tamaño de Poro

Designation: D4641 – 94 (Reapproved 2006)

Standard Practice for Calculation of Pore Size Distributions of Catalysts from Nitrogen Desorption Isotherms[1]

This standard is issued under the fixed designation D4641; the number immediately following the designation indicates the year of original adoption or, in the case of revision, the year of last revision. A number in parentheses indicates the year of last reapproval. A superscript epsilon (ε) indicates an editorial change since the last revision or reapproval.

1. Scope

1.1 This practice covers the calculation of pore size distributions for catalysts and catalyst carriers from nitrogen desorption isotherms. The computational procedure is particularly useful for determining how the pore volume is distributed in catalyst samples containing pores whose sizes range from approximately 1.5 to 100 nm (15 to 1000 Å) in radius. It should be used with caution when applied to isotherms for samples containing pores both within this size range and pores larger than 100 nm (1000 Å) in radius. In such instances the isotherms rise steeply near $P/P_o = 1$ and the total pore volume cannot be well defined. The calculations should be begun at a point on the isotherm near saturation preferably in a region near $P/P_o = 0.99$, establishing an upper limit on the pore size distribution range to be studied. Simplifications are necessary regarding pore shape. A cylindrical pore model is assumed, and the method treats the pores as non-intersecting, open-ended capillaries which are assumed to function independently of each other during the adsorption or desorption of nitrogen.

NOTE 1—This practice is designed primarily for manual computation and a few simplifications have been made for this purpose. For computer computation, the simplified expressions may be replaced by exact expressions.

1.2 *This standard does not purport to address all of the safety concerns, if any, associated with its use. It is the responsibility of the user of this standard to establish appropriate safety and health practices and determine the applicability of regulatory limitations prior to use.*

2. Referenced Documents

2.1 *ASTM Standards:*[2]

D3766 Terminology Relating to Catalysts and Catalysis

D4222 Test Method for Determination of Nitrogen Adsorption and Desorption Isotherms of Catalysts and Catalyst Carriers by Static Volumetric Measurements

3. Terminology

3.1 *Definitions*—Consult Terminology D3766.

3.2 *Symbols:*

$P_4(i)$	=	pressure after equilibration during desorption, torr.
$P_0(i)$	=	liquid nitrogen vapor pressure, torr.
$V_{d\,r}$	=	see 12.4.10 and 12.5 in Test Method D4222.
$r_k(i)$	=	radius of inner core calculated from Kelvin equation, Å.
T	=	boiling point of nitrogen, K.
V_L	=	liquid nitrogen molar volume at T, cm^3/mole.
γ	=	liquid nitrogen surface tension at T, mN/m.
$\bar{t}(i)$	=	average thickness of the nitrogen film adsorbed on the pore walls, Å .
$r_p(i)$	=	radius of cylindrical pore given by $r_k(i) + t(i)$, Å.
Q	=	volume correction factor defined as $(\bar{r}_p/\bar{r}_k)^2$.
$\Delta V_T(i)$	=	decrease in the amount of nitrogen adsorbed caused by a lowering in relative pressure, mm^3/g.
$\Delta V_f(i)$	=	volume of liquid nitrogen desorbed from pore walls during thinning of the film, mm^3/g.
$\Delta V_k(i)$	=	liquid volume of the inner core in which capillary condensation of the nitrogen occurs, mm^3/g.
$\Delta V_p(i)$	=	liquid volume contained in a group of pores having mean radius $\bar{r}_p$, mm^3/g.
$\Sigma \Delta v_p$	=	cumulative pore volume, mm^3/g.
$\Delta S_p(\bar{i})$	=	area of the pore walls of a cylinder having volume ΔV_p, m^2/g.

4. Summary of Practice

4.1 The pore size distribution is determined by analyzing the desorption data of the nitrogen isotherm. The nitrogen uptake is caused by the multilayer adsorption of a film of nitrogen on the pore walls and by capillary condensation of the nitrogen in the "inner core" regions of the pores. The relative pressure at which filling of the core occurs for a given pore size

[1] This practice is under the jurisdiction of ASTM Committee D32 on Catalysts and is the direct responsibility of Subcommittee D32.01 on Physical-Chemical Properties.

Current edition approved Oct. 1, 2006. Published October 2006. Originally approved in 1987. Last previous edition approved in 1999 as D4641–94(1999)$^{\varepsilon 1}$. DOI: 10.1520/D4641-94R06.

[2] For referenced ASTM standards, visit the ASTM website, www.astm.org, or contact ASTM Customer Service at service@astm.org. For *Annual Book of ASTM Standards* volume information, refer to the standard's Document Summary page on the ASTM website.

by capillary condensation is predicted from the Kelvin equation (1).[3] During desorption, thinning of the multilayer film adsorbed on the pore walls occurs in pores which have previously lost their capillary condensate. Corrections for film thinning are determined by a procedure involving the surface area and radius of the film which becomes exposed as desorption proceeds. In principle, the computational procedure can be applied to either the adsorption branch or desorption branch of the nitrogen isotherm. Unless the presence of ink-bottle shaped pores is suggested by an abrupt closure of the desorption branch on the adsorption branch, the distribution curve derived from the desorption data is preferred, and is described in this procedure. The computational method is essentially the procedure developed by Barrett, Joyner, and Halenda (2) except for the incorporation of a few simplifications.

NOTE 2—In cases where it has been established that the adsorption branch of the nitrogen isotherm is to be analyzed, the procedure proposed by Cranston and Inkley (3) is recommended.

5. Significance and Use

5.1 Pore volume distribution curves obtained from nitrogen sorption isotherms provide one of the best means of characterizing the pore structure in porous catalysts, provided that the limitations of the method are kept in mind. Used in conjunction with the BET treatment for surface area determination (4), these methods provide an indispensable means for studying the structure associated with pores usually important in catalysts. This practice is particularly useful in studying changes in a series of closely related samples caused by treatments, such as heat, compression, or extrusion often used in catalyst manufacturing. Pore volume distribution curves can often provide valuable information during mechanistic studies dealing with catalyst deactivation.

6. Computational Procedure

6.1 This procedure requires the use of a series of experimentally measured relative pressures $[P_d(i)/P_0(i)]$ and the corresponding quantities of nitrogen gas adsorbed $[V_{de}]$ expressed in units of cm^3 STP/g. The experimental data required in the use of this procedure can be measured by following the steps outlined in Test Method D4222. Inspect the nitrogen sorption isotherm in the region above $P/P_o = 0.95$. If the solid contains no pores larger than 100 nm (1000 Å) radius, the isotherm remains nearly horizontal over a range of P/P_o approaching unity and it is a simple matter to select a starting relative pressure within this region, establishing an upper limit on the pore size range to be studied. If pores larger than 100 nm (1000 Å) are present however, the isotherm rises rapidly near $P/P_O = 1$ and the total pore volume cannot be well defined. This limiting adsorption can then be identified reliably only if the temperature is very carefully controlled and there are no "cold spots" in the apparatus (which lead to bulk condensation of the gas and a false measure of the adsorption in the volumetric method). Selecting the starting relative pressure for the computational procedure is then made more difficult. In most cases a starting relative pressure of 0.99 will be suitable, which corresponds to an upper limit on pore size of 100 nm (1000 Å) in radius. If necessary, interpolate the values of V_{de} to determine the quantity of nitrogen gas adsorbed at the chosen starting relative pressure.

6.2 The procedure requires numerous arithmetical steps which can best be carried out with the aid of a work sheet. An example (4) of a form found useful in the calculations is provided in Table 1. List in descending order the experimentally determined relative pressures $[P_d(i)/P_0(i)]$ in Column 1, beginning with the value chosen as the starting relative pressure. Generally, values below a relative pressure of 0.25 will not be required in the calculations. Convert the uptake values into a liquid volume (mm^3/g) by multiplying the value of V_{de} in cm^3 STP/g with the conversion factor 1.5468 derived from $V_L = 34.67$ cm^3/mole. List in Column 9 the corresponding quantities of nitrogen adsorbed.

6.3 For each relative pressure, calculate a value for the radius of the core, r_k, by means of the Kelvin equation,

$$RT \ln (P_d/P_0) = -\frac{2\gamma V_L}{r_k} \qquad (1)$$

given in the form

$$r_k\ (\text{Å}) = -\frac{9.574}{\ln (P_d/P_0)} \qquad (2)$$

with $T = 77.35$ K; $\gamma = 8.88$ mN/m; and $V_L = 34.67$ cm^3/mole. List the values in Column 2. For each successive decrement in relative pressure, calculate $\bar{r}_k$, the mean of the values of r_k for the present and previous pressures, and list these mean values in Column 3.

6.4 The average thickness, t, of the multilayer film of nitrogen adsorbed on the walls of the pores at each relative pressure is used to calculate the amount of nitrogen desorbed from the film in pores which have lost their capillary condensate. For each relative pressure, calculate a value for the film thickness from the expression (5)

$$t\ (\text{Å}) = \left[\frac{13.99}{0.034 - \log (P_d/P_0)}\right]^{\frac{1}{2}} \qquad (3)$$

and list the values in Column 4. For each successive decrement in relative pressure, calculate the differences in the values of t, and list these differences as Δt in Column 5.

6.5 Since a cylindrical pore model is assumed, the radius of the pore, r_p, is given by addition of the core radius, r_k, and the film thickness value, t. Add the values in Column 2 to the corresponding values in Column 4 and record the results in Column 6 as r_p. For each successive decrement in relative pressure, calculate $\bar{r}_p$, the mean of the pore radii, r_p, for the present and previous pressures, and record these values in Column 7.

6.6 Compute the quantity $(\bar{r}_p/\bar{r}_k)^2$ from the values listed in Columns 7 and 3. This quantity will be used later to correct the core volume to the volume for each group of pores. The core volume is the region within the pore that fills by capillary condensation of the nitrogen. List the computed values in Column 8 as the volume correction factor, Q.

[3] The boldface numbers in parentheses refer to a list of references at the end of this standard.

TABLE 1 Pore Distribution Computational Work Sheet

Sample Identification ______________________________ Date______________

1 P_d/P_0	2 r_k Å	3 $\bar{r}_k$ Å	4 t Å	5 Δt Å	6 r_p Å	7 $\bar{r}_p$ Å	8 Q	9 V_{de} mm³/g	10 ΔV_T mm³/g	11 ΔV_f mm³/g	12 ΔV_k mm³/g	13 ΔV_p mm³/g	14 ΔS_p m²/g	15 $\Sigma\Delta S_p$ m²/g	16 $\Sigma\Delta V_p$ mm³/g
		—		—		—	—		—	—	—	—	—	—	
										[xdirc]					

Column 2: $r_k = \dfrac{-9.574}{\ln(P_d/P_0)}$

Column 4: $t = \left[\dfrac{13.99}{0.034 - \log(P_d/P_0)}\right]^{1/2}$

Column 11: $\Delta V_f = 0.085 \cdot \Delta t\ \Sigma\Delta S_p$ (preceding line)

Column 12: $\Delta V_k = \Delta V_T - \Delta V_f$

Column 13: $\Delta V_p = \Delta V_k \times Q$

Column 14: $\Delta S_p = 20 \times (\Delta V_p / \bar{r}_p)$

NOTE 3—For a cylindrical pore $\bar{r}_p$ and $\bar{r}_k$ are related to Q by the exact expression:

$$Q = [\bar{r}_p / (\bar{r}_k + \Delta t)]^2 \qquad (4)$$

For $\bar{r}_k > 30$ Å, $\Delta t < 1$ % $\bar{r}_k$. Simplifying Q by eliminating Δt gives $(\bar{r}_p/\bar{r}_k)^2$.

6.7 The amounts of nitrogen desorbed for each successive decrement in relative pressure are calculated by progressive subtraction of the values of the amounts of nitrogen adsorbed, V_{de}, listed in Column 9 from the succeeding one. Compute these differences and list the values in Column 10 as, ΔV_T. Each value of ΔV_T except for the initial one in line 2 contains contributions from the amounts of nitrogen given up by loss of capillary condensate and by thinning of the nitrogen film adsorbed on the walls of pores which have previously released their capillary condensate. The initial value of ΔV_T is due solely to the amount of nitrogen contributed from loss of capillary condensate, since it is assumed that at the highest relative pressure all of the pores are completely filled with nitrogen, and that no thinning of the nitrogen film occurs for the first decrement in relative pressure.

6.8 In completing the calculation to obtain a value for the pore volume, ΔV_p, corresponding to each mean pore size, $\bar{r}_p$, of a group of pores, it will be necessary to work through the calculation for each line before proceeding to the next line. ΔV_f in Column 11 is the amount of nitrogen given up during desorption from thinning of the nitrogen film adsorbed on pore walls. For line 2, ΔV_f equals zero and the value of ΔV_T is assigned to ΔV_k, the volume of the inner core which fills by capillary condensation of the nitrogen. Multiply the value of ΔV_k by the corresponding volume correction factor, Q, listed in Column 8 to obtain ΔV_p. List the value in Column 13 of line 2.

6.9 Calculate the surface area of the pore walls contained in volume ΔV_p as follows:

$$\Delta S_p\,(\mathrm{m^2/g}) = 20 \times \frac{\Delta V_p}{\bar{r}_p} \qquad (5)$$

Using the value of ΔV_p from Column 13 and the corresponding value of $\bar{r}_p$ from Column 7, compute a value for ΔS_p and list it in Column 14. A value for the total surface area of the pores that have become exposed is obtained by summation of the value for ΔS_p with other ΔS_p values in all preceding lines of Column 14. List the value of total area in Column 15 as $\Sigma\Delta S_p$. A value for the cumulative pore volume is obtained by summation of the value ΔV_p with other ΔV_p values in all preceding lines of Column 13. List the value of the cumulative pore volume in Column 16 as $\Sigma\Delta V_p$.

NOTE 4—The expression relating the surface area of the pore walls contained in volume ΔV_p is as follows:

$$\Delta S_p\,(\mathrm{m^2/g}) = 2 \times \frac{\Delta V_p}{\bar{r}_p} \times 10^4 \qquad (6)$$

with ΔV_p in cubic centimetres and $\bar{r}_p$ in angstroms. Converting cubic centimetres to cubic millimetres gives rise to the conversion factor of 20 in the preceding equation.

6.10 An essential feature of this test method is that the volume of nitrogen lost from the adsorbed multilayer film can be calculated from the total area of the pores exposed, $\Sigma\Delta S_p$, and the decrease in the thickness of the film, Δt. Using the value $\Sigma\Delta S_p$ from the preceding line, compute ΔV_f from the expression

$$\Delta V_f = 0.085 \times \Delta t \times \Sigma\Delta S_p \text{ (preceding line)} \quad (7)$$

and record the value in Column 11. Subtract the value of ΔV_f from ΔV_T to obtain the value of ΔV_k of Column 12. Multiply the value of ΔV_k with the corresponding value of Q in Column 8 to obtain the value of ΔV_p of Column 13. Compute ΔS_p and $\Sigma\Delta S_p$ following the procedure in 6.9. Determine a value for $\Sigma\Delta V_p$.

NOTE 5— See Appendix X1 for a more detailed discussion on the calculation of values for ΔV_f and the source of the coefficient.

6.11 Repeat the calculations in 6.10 for each line down to a relative pressure lying between 0.25 and 0.30. If at an intermediate relative pressure, the value of ΔV_k should become equal to zero or negative, discontinue the calculation, and in all subsequent calculations use the data from the preceding line and above.

NOTE 6—It is generally agreed that the value of the pore size to which the Kelvin equation will no longer apply at the lower end of the pore size range varies from one adsorption system to another. As a result, difficulties arise in knowing precisely where to end the pore volume calculation for a particular nitrogen sorption isotherm. It is believed that the Kelvin equation will rarely be valid for a material below a pore size of 10 to 15 Å. We have chosen to terminate the pore volume calculation at a relative pressure lying between 0.25 and 0.30 which corresponds to pore size within the range from 11.6–13.0Å in radius. There are, however, other procedures that can be used to establish where the calculation should be terminated at the low relative pressure end of the isotherm. These alternative methods include:

(1) The use of the precise value for the relative pressure that corresponds to the closure point of the hysteresis loop at the lower end of the isotherm. This value may represent, in many cases, the point at which irreversible capillary condensation commences within the pore structure of the material.

(2) The use of values of $\Sigma\Delta V_p$ from Column 16 in Table 1 and the value of V_{ds} from line 1 of Column 9. The calculation may be terminated at the point where the value of $\Sigma\Delta V_p$ becomes equal to or greater than the starting value of V_{ds}. At this point in the calculation, the measured pore volume at the chosen starting relative pressure will have been exhausted. If the material is believed to be microporous, this method of termination shall not be used.

(3) A t-plot analysis (5) may be used to detect the beginning of capillary condensation. From a plot of the amounts of nitrogen adsorbed versus the t values determined from the equation in 6.4, the beginning of capillary condensation may be detected from the point of upward curvature in the plot. The relative pressure corresponding to this t value where the upward curvature commences is used to terminate the calculation. This method has the advantage of being able to detect the presence of reversible capillary condensation which is not accompanied by hysteresis and cannot be detected by visual examination of the isotherm. For precise work, this method of termination is highly recommended.

6.12 The last value of $\Sigma\Delta S_p$ computed in Column 15 is assigned to the total cumulative surface area. The last value of $\Sigma\Delta V_p$ computed in Column 16 is assigned to the total cumulative pore volume.

NOTE 7—A comparison of the value for the total cumulative surface area with that for the BET surface area determined from the low pressure region of the isotherm provides an empirical test of the internal consistency of the pore volume distribution calculations. If the assumed pore model is a true representation of the actual pore system, these values should show perfect agreement. Experience has shown that these two values often agree to within ±5 % but differences of ±20 % are not uncommon. If the BET surface area is substantially greater than the total cumulative surface area, the difference may be due to the presence of micropores. Results showing deviations greater than ± 20 % should be interpreted with caution.

7. Presentation of Data

7.1 The report shall consist of the following information:

7.1.1 Sample identification, and a statement indicating the use of the desorption isotherm and a cylindrical pore model.

7.1.2 A table or graph composed of the cumulative pore volume data obtained from the values in Column 16 and the corresponding pore sizes, r_p, given in Column 6. A graphical, cumulative pore volume plot can be constructed by plotting the $\Sigma\Delta V_p$ values in cubic millimetres per gram on the ordinate with an arithmetic scale and the corresponding pore size r_p in Å on the abscissa with a logarithmic or arithmetic scale, as appropriate. This cumulative distribution will generally appear as a smooth line and should reveal points of inflection where the pore volume is changing most rapidly. An example of a cumulative plot is shown in Fig. X1.1.

7.1.3 The report may also include a differential plot of the distribution. This can be constructed from slopes derived from the smoothed cumulative plot at appropriate pore radius intervals (Δr_p' s), or from values of $\Delta V_p/\Delta r_p$ calculated from the data in Columns 6 and 13 of Table 1 and the corresponding values of the mean pore size, $\bar{r}_p$, from Column 7. The change in slope shall be plotted on the ordinate and the corresponding mean pore size on the abscissa. Arithmetic or logarithmic scales may be used on the ordinate and abscissa, as appropriate. An example of a differential plot is shown in Fig. X1.2.

8. Precision and Bias

8.1 This practice determines in suitable cases how the pore volume is distributed as a function of pore size for mesoporous solids. These calculated pore volumes depend on the branch of the nitrogen isotherm used and the pore model assumed. They also vary depending on the precise values used for the film thickness and on how the film thickness corrections are determined. Thus, no statement as to the precision of this practice is possible.

8.2 *Bias*—No estimate of the bias of this practice is possible.

9. Keywords

9.1 catalysts; nitrogen adsorption; pore size distribution

APPENDIX

(Nonmandatory Information)

X1. CALCULATION OF CORRECTIONS FOR THE VOLUME RELEASED DURING THINNING OF THE PHYSICALLY ADSORBED LAYERS

X1.1 According to Barrett, Joyner, and Halenda (2), corrections for the volume of nitrogen lost during the thinning of the adsorbed multilayer film, $\Delta V_f(i)$, are given by the expression:

$$\Delta V_f(i) = \Delta t(i) \sum_{j=1}^{i-1} C(j)\Delta S_p(j) \qquad (X1.1)$$

where:

j = sequence number of desorption steps,

t = adsorbed layer thickness,

$C(j)$ = $\dfrac{(\bar{r}_p(j) - \bar{t}(j))}{\bar{r}_p(j)}$

$\bar{r}_p(j)$ = average pore radius of the pore group emptied in the jth desorption step,

$\bar{t}(j)$ = average adsorbed layer thickness in the jth desorption step, and

$\Delta S_p(j)$ = surface area of the pore group emptied in the jth desorption step.

X1.2 See Fig. X1.1 and Fig. X1.2. The value of C varies for the different pore groups, and since t is a function of relative pressure, the value of C for a particular pore group varies stepwise with relative pressure. These variations in the C values make the calculation of ΔV_f from the above expression very time consuming. In practice, it has been shown (2) that a very close approximation to the correct pore size distribution can be obtained by using a constant C value for a particular adsorbent. Since the C value is known to vary between the limits (2) of 0.72 to 0.97 for pores of any size, we have chosen a value of 0.85 which is midway between the limits of C in deriving the equation for ΔV_f in 6.10. Other constant values of C may be used in place of 0.85 by substituting the selected C value into the equation

$$\Delta V_f = C \times 0.1 \times \Delta t \times \Delta S_p \text{ (preceding line)} \qquad (X1.2)$$

and replacing the equation in 6.10 with the above. For precise work, it is recommended that the value of C be allowed to vary. This will require the redetermination of the C value for each pore group at the various relative pressures used in the computation.

NOTE X1.1—Because of the time and effort involved in the use of variable C values, it is desirable to facilitate the computations with the aid of a computer.

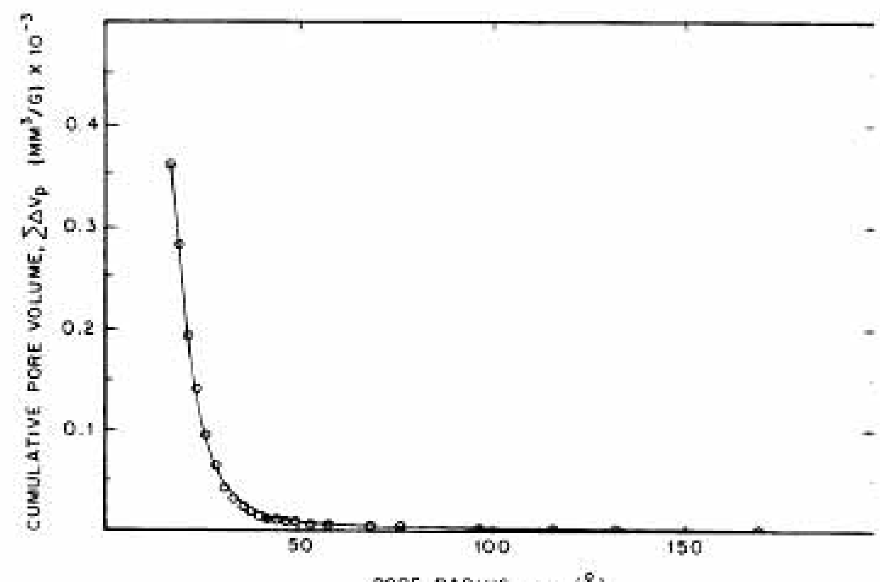

FIG. X1.1 Example of Cumulative Pore Volume Plot on a Silica-Alumina Cracking Catalyst

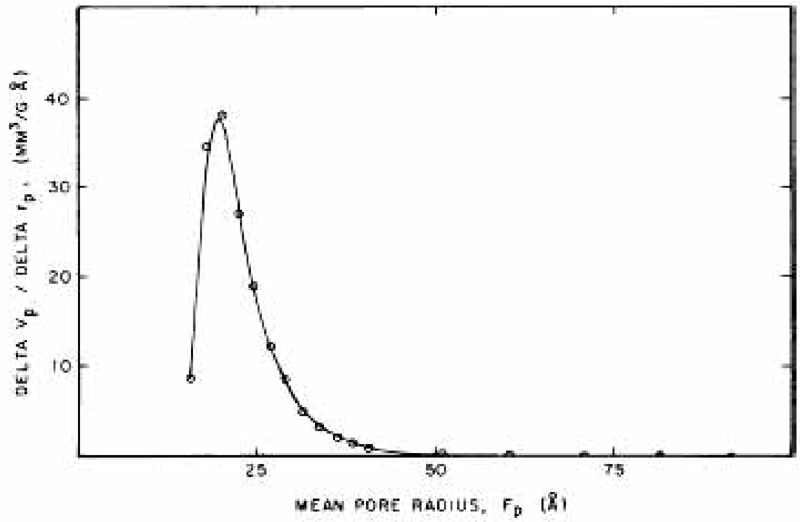

FIG. X1.2 Example of a Differential Plot on a Silica-Alumina Cracking Catalyst

REFERENCES

(1) Thompson, W. T., *Philosophical Magazine*, Vol 42, 1871, p. 448.
(2) Barrett, E. P., Joyner, L. G., and Halenda, P. P., *Journal American Chemistry Society*, Vol 73, 1951, p. 373.
(3) Cranston, R. W., and Inkley, F. A., "Advances in Catalysis," Vol 9, p 143. Academic Press, New York and London, 1957.
(4) Gregg, S. J., and Sing, K. S. W., "Adsorption, Surface Area and Porosity," 2nd Ed., Academic Press, New York and London, 1982, pp. 44, 137.
(5) de Boer, J. H., Lippens, B. C., Linsen, J. C., Broekhoff, P., van den Heuvel, A., and Osinga, Th. J., *Journal of Coll. Int. Science*, Vol 21, 1966, p. 405.

Bibliografía

AKERHOLM, M. Ultrastructural Aspects of Pulp Fibers as Stugdied by Dynamic FT-IR Spectroscopy. Swedish Pulp and Paper Research Institute. Stockholm, Royal Institute of Technology. 2003

AKERHOLM, M., HINTERSTOISSER, B. y SALMÉN, L. Characterization of the crystalline structure of cellulose using static and dynamic FT-IR spectroscopy. Carbohydrate Research. vol. 339, pág. 569-578. 2004.

AMMON, H., EGE, W., y col. Improvement in the long-term stability of an amperometric glucose sensor system by introducing a cellulose membrane of bacterial origin. Analytical Chemistry. vol. 67(2), pág. 466-471. 1995.

ANDRADE, F., COSTA, R., y col. Improving bacterial cellulose for blood vessel replacement: Functionalization with a chimeric protein containing a cellulose-binding module and an adhesion peptide. Acta Biomaterialia. vol. 6(10), pág. 40344041. 2010.

ANGULO, C., BONILLA, A. y BOYACÁ, A. Estudio y evaluación de la síntesis de una membrana polimérica para pervaporación de un sistema de esterificación. Tesis para la obtención del título de Ingeniero Químico.. Departamento de Ingeniería Química. Bogotá, Universidad Nacional de Colombia. 2003

ARAQUE, M. Módulo Básico de Catálisis Heterogénea. Tesis para la obtención de grado de Ingeniero Químico. Departamento de Ingeniería Química. Bogotá, Universidad Nacional de Colombia. 2003

ASTLEY, O., CHANLIAUD, E., y col. Tensile deformation of bacterial cellulose composites. International Journal of Biological Macromolecules. vol. 32, pág. 28–35. 2003.

ASTM D3663-03. Standard Test Method for Surface Area of Catalysts and Catalyst Carriers. ASTM International. 2008.

ASTM D4641-94. Standard Practice for Calculation of Pore Size Distributions of Catalysts from Nitrogen Desorption Isotherms. ASTM International. 2006.

ATKINSON, S. US Membrane Separation Technology Markets Analyzed. Membrane Technology. vol. 2002(9), pág. 10-12. 2002.

AVILA, G. y CAICEDO, L. Estudio cinético de la producción de exopolisacáridos empleando un cultivo mixto del hongo del té. Tesis para la obtención de grado de Magíster en Ingeniería Química. Departamento de Ingeniería Química. Bogotá, Universidad Nacional de Colombia. 2007.

BÄCKDAHLA, H., HELENIUS, G., y col. Mechanical properties of bacterial cellulose and interactions with smooth muscle cells. Biomaterials vol. 27, pág. 2141–2149. 2006.

BAE, S. y SHODA, M. Production of bacterial cellulose by Acetobacter xylinum BPR2001 using molasses medium in a jar fermentor. Applied Microbial Biotechnology vol. 67, pág. 45-51. 2005a.

BAE, S. y SHODA, M. Statistical Optimization of Culture Conditions for Bacterial Cellulose Production Using Box-Behnken Design. Biotechnology and Bioengineering. vol. 90, pág. 20-28. 2005b.

BAE, S., SUGANO, Y. y SHODA, M. Improvement of Bacterial Cellulose Production by addition of agar in a Jar Fermentor. Journal of Bioscience and Bioengineering. vol. 97 (1), pág. 33-38. 2004.

BAKER, R. Overview of Membrane Science and Technology. 2nd Ed. 2004.

BALMANN, H. y NOBREGA, R. The Deformation of Dextran molecules: Causes and consequences in ultrafiltration. Journal of Membrane Science. vol. 40(3), pág. 311-327. 1989.

BANAT, F., AL-RUB, F., y col. Application of Stefan-Maxwell approach to azeotropic separation by membrane distillation. Chemical Engineering Journal. vol. 73 pág. 71-75. 1999.

BARANOV, A., ANISIMOVA, V., y col. Dielectric properties and dipole glass transition in cellulose Acetobacter xylinum. Ferroelectrics. vol. 289, pág. 141-151. 2003.

BARBOSA, M. y MORENO, N. Producción de polihidroxialcanoatos (PHAs) empleando Ralstonia eutropha. Tesis para la obtención del título de Ingeniero Químico. Departamento de Ingeniería Química. Bogotá, Universidad Nacional de Colombia. 2002

BASTA, A. y EL-SAIED, H. Performance of improved bacterial cellulose application in the production of functional paper. Journal of Applied Microbiology. vol. 107(6), pág. 2098-2107. 2009.

BELBEKHOUCHE, S., BRAS, J., *et al.* Water sorption behavior and gas barrier properties of cellulose whiskers and microfibrils films. Carbohydrate Polymers. vol. 83(4), pág. 1740-1748. *2011*.

BEN-HAYYIM, G. y OHAD, I. Synthesis of Cellulose by Acetobacter xylinum VIII. On the formation and Orientation of Bacterial Cellulose Fibrils in the Presence of Acidic Polysaccharides. Journal of Cell Biology. vol. 25(2), pág. 191-207. 1965.

BERTOCCHI, C., DELNERI, D., y col. Characterization of microbial cellulose from a high-producing mutagenized Acetobacter pasteurianus strain. Biochimica et Biophysica Acta vol. 1336 pág. 211–217. 1997.

BERTRANM, M., DALE, B. Determination of Cellulose Accesibility by DSC. Journal of Applied Polymer Science. vol. 32, pág. 4241-4253. 1986.

BIELECKI, S., KRYSTYNOWICZ, A., y col. Bacterial Cellulose. Biopolymers. vol. 5(3), pág. 40-85. 2002.

BORZANI, W. y DE SOUZA, S. Mechanism of the film thickness increasing during the Bacterial production of Cellulose on non-agitated liquid media. Biotechnology Letters. vol. 17 (11), pág. 1271-1272. 1995.

BRACKMANN, C., BODIN, A., y col. Visualization of the cellulose biosynthesis and cell integration into cellulose scaffolds. Biomacromolecules. vol. 11(3), pág. 542-548. 2010.

BUDHIONO, A., ROSIDI, B., y col. Kinetic aspects of Bacterial Cellulose formation in nata-de-coco- culture system. Carbohydrate polymers vol. 40, pág. 137–143. 1999.

BUYANOV, A., GOFMAN, I., y col. Anisotropic swelling and mechanical behavior of composite bacterial cellulose-poly(acrylamide or acrylamide-sodium acrylate) hydrogels. Journal Of The Mechanical Behavior Of Biomedical Materials. vol. 3(1), pág. 102-111. 2010.

CAI, Z., JIN, H. y KIM, J. Chitosan blended bacterial cellulose as a smart material for biomedical application. Proceedings of SPIE - The International Society for Optical Engineering. 2009.

CAICEDO, L., DE FRANÇA, F. y DE ALMEIDA, L. A Produção de Celulose Bacteriana em Reatores de Tambor Rotatório. Tesis para la obtención de grado de Doctor en Ciencias. Escola de Química. Río de Janeiro, Universidade Federal do Rio de Janeiro. 2002.

CAICEDO, L., DE FRANCA, F., y col. Permeabilidad hidráulica e hinchamiento en membranas de celulosa bacteriana. Memorias, III Congreso Internacional de Biomateriales BIOMAT. 2003.

CAICEDO, L., DE FRANCA, F. y LOPEZ, L. Factores para el escalado del proceso de producción de celulosa por fermentación estática. Revista Colombiana de Química. vol. 30 (2), pág. 155-162. 2001.

CARREÑO, L. y CAICEDO, L. Producción de Membranas de Celulosa Bacteriana a Partir de Diferentes Fuentes de Carbono. II Simposio sobre Biofábricas. Medellín, Colombia. 2005.

CASTRO, G., CAICEDO, L., y col. Solvent extraction of organic acids from stillage for its re-use in ethanol production process. Waste management & Research. vol 28, (6), pág. 533-538, 2010.

CIECHAŃSKA, D., STRUSZCZYK, H., y col. New electro-acoustic transducers based on modified bacterial cellulose. Fibres and Textiles in Eastern Europe. vol. 10(1), pág. 27-30. 2002.

CLASEN, C., SULTANOVA, B., y col. Effects of Different Drying Processes on the Material Properties of Bacterial Cellulose Membranes. Macromolecular Symposia. vol. 244, pág. 48-58. 2006.

CONCARO, S., AASE, B., y col. Bacterial cellulose as a potential material for meniscal tissue engineering. Osteoarthritis and Cartilage. vol. 15(Supplement 2), pág. B75-76. 2007.

CZAJA, W., KRYSTYNOWICZ, A. y BIELECKI, S., BROWN, R. Microbial cellulose: the natural power to heal wounds. Biomaterials vol. 27, pág. 145-151. 2006.

CZAJA, W., ROMANOVICZ, D. y BROWN, R. Structural investigations of microbial cellulose produced in stationary and agitated culture. Cellulose. vol. 11, pág. 403-411. 2004.

CZAJA, W., YOUNG, D., y col. The Future Prospects of Microbial Cellulose in Biomedical Applications. Biomacromolecules. vol. 8(1). 2007.

CHAO, Y., MIRATAI, M., y col. Effect of addition of water-soluble polysaccharides on bacterial cellulose production in a 50- L Airlift Reactor. Biotechnology Progress. vol. 17 pág. 781-785. 2001.

CHARPENTIER, P., MAGUIRE, A. y WAN, W. Surface modification of polyester to produce a bacterial cellulose- based vascular prosthetic device. Applied Surface Science. vol. 252, pág. 6360-6367. 2006.

CHAWLA, P., BAJAJ, I., y col. Microbial Cellulose: Fermentative Production and Applications. Food Technology and Biotechnology. vol. 47(2), pág. 107-124. 2009.

CHENG, H., WANG, P., y col. Cultivation of Acetobacter xylinum for bacterial cellulose production in a modified airlift reactor. Biotechnology and Applied Biochemistry. vol. 35, pág. 125–132. 2002.

CHENG, K., CATCHMARK, J. y DEMIRCI, A. Effect of different additives on bacterial cellulose production by Acetobacter xylinum and analysis of material property. Cellulose. vol. 16(6), pág. 1033-1045. 2009a.

CHENG, K., CATCHMARK, J. y DEMIRCI, A. Enhanced production of bacterial cellulose by using a biofilm reactor and its material property analysis. Journal of Biological Engineering. vol. 3(1), pág. 12. 2009b.

DAMMSTRÖM, S., SALMÉN, L. y GATENHOLM, P. The effect of moisture on the dynamical mechanical properties of bacterial cellulose/glucuronoxylan nanocomposites. Polymer. vol. 46, pág. 10364–10371. 2005.

DUARTE, A., PINO, J. y CAICEDO, L. Estudio sobre el efecto de la fuente de carbono y la aireación sobre la producción de ácido itacónico por fermentación. Ed Universidad Nacional de Colombia. Bogotá. 1995.

DUDMAN, W. Cellulose Production by Acetobacter acetigenum and other Acetobacter spp. Journal of General Microbiology. vol. 21, pág. 312-326. 1959.

DUVEY, V., SAXENA, C., y col. Pervaporation of binary water–ethanol mixtures through bacterial cellulose membrane. Separation and Purification Technology. vol. 27, pág. 163-171. 2002.

DUVEY, V., PANDEY, L. y SAXENA, C. Pervaporative separation of ethanol/water azeotrope using a novel chitosan-impregned bacterial cellulose membrane and chitosan-poly(vinil alcohol) blends. Journal of Membrane Science vol. 251, pág. 131-136. 2005.

ELNAGHY, M., MEGALIA, S. Gluconic Acid Production by *Penicilium puberulum*. Folia Microbiologica. Vol. 20(6), pág. 504-508. 1975.

EMBUSCADO, M., MARKS, J. y BEMILLER, J. Bacterial cellulose. I. Factors affecting the production of cellulose by Acetobacter xylinum. Food Hydrocolloids. vol. 8(5), pág. 407-418. 1994a.

EMBUSCADO, M., MARKS, J. y BEMILLER, J. Bacterial cellulose. II. Optimization of cellulose production by Acetobacter xylinum through response surface methodology. Food Hydrocolloids. vol. 8(5), pág. 419-430. 1994b.

EVANS, B., O´NEILL, H., y col. Palladium-bacterial cellulose membranes for fuel cells. Biosensors and Bioelectronics vol. 18, pág. 917-992. 2003.

FESTUCCI-BUSELLI, R., OTONI, W. y JOSHI, C. Structure, organization, and functions of cellulose synthase complexes in higher plants. Brazilian Journal of Plant Physiology. vol. 19(1), pág. 1-13. 2007.

FONTANA, J., DE SOUZA, A., y col. Acetobacter Cellulose Pellicle as a Temporary Skin Substitute. Applied Biochemistry and Biotechnology. vol. 24/25, pág. 253-263. 1990.

FREDONIA, G. Membrane Separation Technologies. US Industry Study with Forecasts to 2010 & 2015. Cleveland, OH, The Fredonia Group. 2006.

GEORGE, J., RAMANA, K., y col. Physico-mechanical properties of chemically treated bacterial (Acetobacter xylinum) cellulose membrane World Journal of Microbiology and Biotechnology vol. 21, pág. 1323-1327. 2005a.

GEORGE, J., RAMANA, K., y col. Characterization of chemically treated bacterial (Acetobacter xylinum) biopolymer: Some thermo-mechanical properties. International Journal of Biological Macromolecules. vol. 37, pág. 189-194. 2005b.

GHOREYSHI, S., FARHADPOUR, F. y SOLTANIEH, M. Multicomponent transport across nonporous polymeric membranes. Desalination. vol. 144, pág. 93-101. 2002.

GÓMEZ, A., GUZMAN, D. y BOADA, L. Síntesis y caracterización de una membrana para perevaporación de un sistema etanol-agua. Tesis para la obtención del título de Ingeniero Químico. Departamento de Ingeniería Química. Bogotá, Universidad Nacional De Colombia. 2003

GOSTING, L. y XKELEY, D. A Study of the Diffusion of Urea in Water at 25°C with the Gouy Interference Method. Journal of the American Chemical Society. vol. 74(8), pág. 2058-2060. 1952.

GRANDE, C., TORRES, F., y col. Nanocomposites of bacterial cellulose/hydroxyapatite for biomedical applications. Acta Biomaterialia. vol. 5(5), pág. 1605-1615. 2009.

GROMET, Z., SCHRAMM, M. y HESTRIN, S. Synthesis of Cellulose by Acetobacter xylinum. 4. Enzyme Systems Present in a Crude Extract of Glucose-Grown Cells. Biochemical Journal. vol. 67, pág. 679-689. 1957.

GUEVARA, R. Efecto de la velocidad de agitación y la aireación en la producción de ácido acético y biopolimero en fermentación sumergida con el hongo del té. Tesis para la obtención del título de Ingeniero Químico. Departamento de Ingeniería Química. Bogotá, Universidad Nacional de Colombia. 1994.

HABE, H., SHIMADA, Y., y col. Production of Glyceric Acid by Gluconobacter sp. NBRC 3259 Using Raw Glycerol. Bioscience, Biotechnology and Biochemistry. vol. 73(8), pág. 1799-1805. 2009.

HABE, H., SHIMADA, Y., y col. Use of Gluconobacter frateurii Mutant to Prevent Dihydroxyacetone Accumulation During Glyceric Acid Production from Glycerol. Bioscience, Biotechnology and Biochemistry. vol. 74(11), pág. 2330-2332. 2010.

HABERT, A., BORGES, C. y NOBREGA, R. Processos de Separação por Membranas. Río de Janeiro, e-papers. 2006.

HAN, N. y ROBYT, F. The mechanism of Acetobacter xylinum celullose biosynthesis: direction of chain elongation and the role of lipid pyrophosphate intermediates in the cell membrane. Carbohydrate Research. vol. 313, pág. 125-133. 1998.

HEINTZ, A. y STEPHAN, W. A generalized solution—diffusion model of the pervaporation process through composite membranes Part II. Concentration polarization, coupled diffusion and the influence of the porous support layer. Journal of Membrane Science. vol. 89, pág. 153-169. 1994.

HESTRIN, S. y SCHRAMM, M. Synthesis of cellulose by Acetobacterxylinum. II. Preparation of freeze-dried cells capable of polymerizing glucose to cellulose. Biochemical Journal. vol. 58, pág. 345-352. 1954.

HIRAI, A., HORII, F. y KITAMARU, R. Transformation of Native Cellulose Crystals from Ia to Ib through Solid- State chemical reactions. Macromolecules vol. 20, pág. 1440-1442. 1987.

HIRAI, A., TSUJI, M. y HORII, F. Culture Conditions Producing Structure entities Composed of Cellulose I and II in Bacterial Cellulose. Cellulose vol. 4, pág. 239-245. 1997.

HIRAI, A., TSUJI, M., et al. In situ crystallization of bacterial cellulose III. Influences of different polymeric additives on the formation of microfibrils as revealed by tranmission electron microscopy. Cellulose vol. 5, pág. 201-213. 1998.

HIRAI, A., TSUJI, M. y HORII, F. TEM study of band-like cellulose assemblies produced by Acetobacter xylinum at 4 °C. Cellulose. vol. 9(105), pág. 113. 2002.

HOLLMAN, A. y BHATTACHARYYA, D. Controlled Permeability and Ion Exclusion in Microporous Membranes Functionalized with Poly(L-glutamic acid). Langmuir. vol. 18, pág. 5946-5952. 2002.

HONG, L., WANG, Y., y col. Hydroxyapatite/bacterial cellulose composites synthesized via a biomimetic route. Materials Letters. vol. 60(13-14), pág. 1710-1713. 2006.

HORII, F., KAJI, H., y col. Cellulose Assemblies Produced by *Acetobacter xylinum*. ICR Annual Report. 1999.

HORNUNG, M., LUDWIG, M., y col. Optimizing the Production of Bacterial Cellulose in Surface Culture: Evaluation of Substrate Mass Transfer Influences on the Bioreaction (Part 1). Engineering in Life Sciences. vol. 6(6), pág. 537-545. 2006.

HULT, E., YAMANAKA, S., y col. Aggregation of ribbons in Bacterial Cellulose induced by high pressure incubation. Carbohydrate Polymers vol. 53, pág. 9-14. 2003.

HWANG, J., YANG, Y., y col. Effects of pH and Dissolved Oxygen on Cellulose Production by Acetobacter xylinum BRC5 in Agitated Culture. . Journal of Bioscience and Bioengineering vol. 88, pág. 183-188. 1999.

HWANG, S. Nonequilibrium Thermodynamics to Membrane Transport. AIChE Journal. vol. 50, pág. 862-870. 2004.

ISHIDA, T., SUGANO, Y., y col. Effects of Acetan on Poduction of Bacterial Cellulose by Acetobacter xylinum. Bioscience, Biotechnology, Biochemistry vol. 66, pág. 1677-1681. 2002.

ISHIHARA, M., MATSUNAGA, M., y col. Utilization of D- xylose as carbon source for production of bacterial cellulose. Enzyme and Microbial Technology. vol. 31, pág. 986-991. 2002.

IWATA, T., INDRARTI, L. y AZUMA, J. Affinity of hemicellulose for cellulose produced by Acetobacter xylinum. Cellulose vol. 5, pág. 215-228. 1998.

IZÁK, P., BARTOVSKÁ, L., y col. Description of binary liquid mixtures transport through non-porous membrane by modified Maxwell–Stefan equations. Journal of Membrane Science. vol. 214, pág. 293-309. 2003.

JIA, H., JIA, Y., y col. Potentiality of bacterial cellulose as the scaffold of tissue engineering of cornea. Proceedings of the 2009 2nd International Conference on Biomedical Engineering and Informatics, BMEI 2009, art. no. 5305657. vol. 2009.

JIA, H., JIA, Y., y col. Method to construct tissue engineering corneal stroma with bacterial cellulose and its evaluation. Journal of Jilin University Medicine Edition. vol. 36(2), pág. 303-307. 2010.

JIE, X., CAO, Y., y col. Influence of drying method on morphology and properties of asymmetric cellulose hollow fiber membrane. Journal of Membrane Science. vol. 246, pág. 157-165. 2005.

JONAS, R. y FARAH, L. Production and applications of microbial cellulose. Polymer Degradation vol. 59, pág. 101-106. 1998.

JOSEPH, G., ROWE, G., y col. Effects of Polyacrylamide-co-acrylic acid on cellulose production by Acetobacter xylinum. Journal of Chemical Technology and Biotechnology vol. 78, pág. 964-970. 2003.

JUNG, H., JEONG, J., y col. Influence of glycerol on production and structural-physical properties of cellulose from Acetobacter sp. V6 cultured in shake flasks. Bioresource Technology. vol. 101(10), pág. 3602-3608. 2010.

JUNG, J., PARK, J. y CHANG, H. Bacterial cellulose production by Gluconacetobacter hansenii in an agitated culture without living non-cellulose producing cells. Enzyme and Microbial Technology vol. 37, pág. 347–354. 2005.

KACURAKOVA, M., SMITH, A., y col. Molecular interactions in bacterial cellulose composites studied by ID FT-IR and dynamic 2D FT-IR spectroscopy. Carbohydrate Research vol. 337, pág. 1145-1153. 2002.

KERKHOF, P. A modified Maxwell-Stefan model for transport through to inert membranes: The binary friction model. The Chemical Engineering Journal. vol. 64, pág. 319-343. 1996.

KESHK, S. y SAMESHIMA, K. Evaluation of different carbon sources for bacterial cellulose production. African Journal of Biotechnology. vol. 4, pág. 478-482. 2005.

KESHK, S., RAZEK, T. y SAMESHIMA, K. Bacterial Cellulose Production from Beet Molasses. African Journal of Biotechnology. vol. 5(17), pág. 1519-1523. 2006a.

KESHK, S. Physical properties of Bacterial Cellulose sheets produced in presence of lignosulfonate. Enzyme and Microbial Technology vol. 40, pág. 9-12. 2006b.

KESHK, S. y SAMEJIMA, M. The utilization of sugar cane molasses with/without the presence of lignosulfonate for the production of bacterial cellulose. Applied Microbiology and Biotechnology. vol. 72, pág. 291-296. 2006c.

KIM, D., NISHIYAMA, Y. y KUGA, S. Surface acetylation of bacterial cellulose. Cellulose. vol. 9, pág. 361-367. 2002.

KLEMM, D., SCHUMANN, D., y col. Bacterial synthesized cellulose - artificial blood vessels for microsurgery. Progress in Polymer Science vol. 6, pág. 1561-1603. 2001.

KLOPFFER, M. y FLACONNÈCHE, B. Transport Properties of Gases in Polymers: Bibliographic Review. Oil & Gas Science and Technology – Rev. IFP. vol. 56(3), pág. 223-244. 2001.

KOUDA, T., YANO, H., y col. Characterization of Non-Newtonian Behavior During Mixing of Bacterial Cellulose in a Biorreactor. Journal of Fermentation and Bioengineering vol. 82, pág. 382-386. 1996.

KOUDA, T., NARITOMI, T., et al. Effects of oxygen and carbon dioxide pressures on bacterial cellulose production by Acetobacter in aerated and agitated culture. Journal of Fermentation and Bioengineering. vol. 84(2), pág. 124-127. 1997a.

KOUDA, T., YANO, H. y YOSHINAGA, F. Effect of Agitator Configuration on Bacterial Cellulose Productivity in Aerated and Agitated Culture. Journal of Fermentation and Bioengineering. vol. 83, pág. 371-376. 1997b.

KRISHNA, R. y STANDART, G. A multicomponent film model incorporating a general matrix method of solution to the Maxwell-Stefan equations. AiChE Journal. vol. 22, pág. 383-389. 1976.

KRYSTYNOWICZ, A., BIELECKI, S., y col. Application of bacterial cellulose for clarification of fruit juices. Progress in Biotechnology, Elsevier Science B.V. vol, pág. 2000.

KUMANO, A. y FUJIWARA, M. Cellulose Triacetate Membranes for Reverse Osmosis. Advanced Membrane Technology and Applications. Hoboken, New Jersey, Wiley & Sons Inc. vol, pág. 2008.

KUROSUMI, A., SASAKI, C., y col. Utilization of various fruit juices as carbon source for production of bacterial cellulose by Acetobacter xylinum NBRC 13693. Carbohydrate Polymers. vol. 76, pág. 333-335. 2009.

KUZNETSOVA, E. A New Method for Describing the Concentration Dependence of the Diffusion Coefficients of Strong Electrolytes in Aqueous Solutions at 298.15 K. Russian Journal of Physical Chemistry A. vol. 81(8), pág. 1234–1241. 2007.

LEGNANI, C., VILANI, C., y col. Bacterial cellulose membrane as flexible substrate for organic light emitting devices. Thin Solid Films. vol. 517(3), pág. 1016-1020. 2008.

LI, J., WAN, Y., y col. Preparation and characterization of 2,3-dialdehyde bacterial cellulose for potential biodegradable tissue engineering scaffolds. Materials Science and Engineering C. vol. 29(5), pág. 1635-1642. 2009a.

LI, F., ZHU, C., y col. In vivo evaluation of the biocompatibility of tissue-engineered tubular nanometer bacterial cellulose. Chinese Journal of Biomedical Engineering vol. 28(5), pág. 760-765. 2009b.

LI, X., CHEN, S., y col. In situ synthesis of CdS nanoparticles on bacterial cellulose nanofibers. Carbohydrate Polymers. vol. 76(4), pág. 509-512. 2009c.

LONSDALE, H. The Growth of Membrane Technology. Journal of Membrane Science. vol. 10, pág. 81-181. 1982.

LUCENA, E., ORTIZ, Z. y BOYACÁ, A. Síntesis de una membrana polimérica para perevaporación. Tesis para la obtención del título de Ingeniero Químico. Departamento de Ingeniería Química. Bogotá, Universidad Nacional de Colombia. 1999.

LLOYD, A. Bacterial cellulose scaffolds for cartilage repair: Tissue engineering. Materials Today. vol. 7(11), pág. 28-2413. 2004.

MANEERUNG, T., TOKURA, S. y RUJIRAVANIT, R. Impregnation of silver nanoparticles into bacterial cellulose for antimicrobial wound dressing. Carbohydrate Polymers. vol. 72(1), pág. 43-51. 2008.

MARTÍN, J. Adsorción Física de Gases y Vapores por Carbones, Universidad de Alicante. 1990.

MARX-FIRGINI, M. y PION, B. Kinetic invetigations of biosynthesis of cellulose by Actobacter xylinum. Biochimica et Biophysica Acta (BBA) - General Subjects. vol. 338(2), pág. 382-393. 1974.

MATHEWS, J., SKOPEC, C., y col. Computer Simulation studies of microcrystalline cellulose Ib. Carbohydrate Research vol. 341, pág. 138-152. 2006.

MATSUOKA, M., TSUCHIDA, T., y col. A Synthetic Medium for Bacterial Cellulose Production by Acetobacter xylinum subsp. Sucrofermentans. Bioscience, Biotechnology, Biochemistry vol. 60, pág. 575-579. 1996.

MIKKELSEN, D., FLANAGAN, B., y col. Influence of different carbon sources on bacterial cellulose production by Gluconacetobacter xylinus strain ATCC 53524. Journal of Applied Microbiology. vol. 107(2), pág. 576-583. 2009.

MIRANDA, C., PIACSEK, C. y FERREIRA, E. Desenvolvimento de Membranas de Osmose Inversa Resistentes à Deposição de Matéria Orgânica e Bioincrustações. Tesis para la obtención del grado de Doctor en Ciencias. COPPE/PEQ Universidad Federal de Río de Janeiro. 2009.

MONCADA, E. y BOYACÁ, A. Estandarización de condiciones de operación de un módulo de perevaporación. Tesis para la obtención del título de Magíster en Ingeniería Química. Departamento de Ingeniería Química. Bogotá, Universidad Nacional de Colombia. 2004.

MUKAI, M., TATSUMI, D. y MATSUMOTO, T. Evaluation of bacterial cellulose membrane for fuel cells Polymer Preprints, Japan. vol. 55(2), pág. 4820. 2006.

NARITOMI, T., KOUDA, T., y col. Effect of Ethanol on Bacterial Cellulose Production from Fructose in Continuous Culture. Journal of Fermentation and Bioengineeering. vol. 85(6), pág. 598-603. 1998a.

NARITOMI, T., KOUDA, T., y col. Effect of Lactate on Bacterial Cellulose Production from Fructose in Continuous Culture. Journal of Fermentation and Bioengineering. vol. 85 (1), pág. 89-95. 1998b.

NARITOMI, T., KOUDA, T., y col. Inhibitory Effect of Carbon Dioxide on Bacterial Cellulose Production by Acetobacter in Agitated Culture. Journal of Fermentation and Bioengineeering. vol. 85(3), pág. 318-321. 1998c.

NISHI, N., URYU, M., y col. The Structure and Mechanical Properties of Sheets Prepared fromm Bacterial Cellulose. Part 2. Improvement of the mechanical Properties of sheets and their applicability to diaphragms of electroacoustic transducers. Journal of Materials Science. vol. 25, pág. 2997-3001. 1990.

NWE, N., FURUIKE, T. y TAMURA, H. Selection of a biopolymer based on attachment, morphology and proliferation of fibroblast NIH/3T3 cells for the development of a biodegradable tissue regeneration template: Alginate, bacterial cellulose and gelatin. Process Biochemistry. vol. 45(4), pág. 457-466. 2010.

O´SULLIVAN, A. Cellulose: The structure slowly unravels. Cellulose. vol. 4, pág. 173-207. 1997.

OIKAWA, T., OHTORI, T. y AMEYAMA, M. Production of Cellulose from D-Arabitol by Acetobacter xylinum KU-1. Bioscience, Biotechnology and Biochemistry. vol. 59(8), pág. 1564-1565. 1995a.

OIKAWA, T., OHTORI, T. y AMEYAMA, M. Production of cellulose from D.mannitol by Acetobacter xylinum KU-1. Bioscience, Biotechnology, Biochemistry. vol. 59(2), pág. 331-332. 1995b.

OKAMOTO, T., YAMANO, S., y col. Cloning of the Acetobacter xylinum cellulase gene and its expression in Escherichia coli and Zymomonas mobilis. Applied Microbiology and Biotechnology. vol. 42(4), pág. 563-568. 1994.

OUGIYA, H., WATANABE, K., y col. Emulsion-stabilizing Effect of Bacterial Cellulose. Bioscience, Biotechnology and Biochemistry. vol. 61(9), pág. 1541-1545. 1997.

OUGIYA, H., WATANABE, K., y col. Relationship between Suspension Properties and Fibril Structure of Disintegrated Bacterial Cellulose. Bioscience, Biotechnology, Biochemistry. vol. 62(9), pág. 1714-1719. 1998.

PANDEY, L., SAXENA, C. y DUVEY, V. Studies on pervaporative characteristics of bacterial cellulose membrane. Separation and Purification Technology. vol. 42, pág. 213-218. 2005.

PHARMACOSMOS "Physical Properties of Dextran." http://www.dextran.net/dextran-physical-properties.html, 2011.

PHISALAPHONG, M. y JATUPAIBOON, N. Biosynthesis and Characterization of Bacteria Cellulose-Chitosan Film. Carbohydrate Polymers. 2008.

PLAZA, J., ZOQUE, L. y BOYACÁ, A. Estudio del empleo de la pervaporación en la concentración de sistemas etanol - agua. Tesis para la obtención del título de Ingeniero Químico. Departamento de Ingeniería Química. Bogotá, Universidad Nacional de Colombia. 2000.

POURRAMEZAN, G., ROAYAEI, A. y QEZELBACH, Q. Optimization of Culture Conditions for Bacterial Cellulose Production by Acetobacter sp.4B-2. Biotechnology. vol. 8(1), pág. 150-154. 2009.

RAMANA, K., TOMAR, A. y SINGH, L. Effect of various carbon and nitrogen sources on cellulose synthesis by Acetobacter xylinum. World Journal of Microbiology and Biotechnology vol. 16, pág. 245-248. 2000.

RAMBO, C., RECOUVREUX, D., y col. Template assisted synthesis of porous nanofibrous cellulose membranes for tissue engineering. Materials Science and Engineering C. vol. 28, pág. 549-554. 2008.

RETEGI, A., GABILONDO, N., y col. Bacterial cellulose films with controlled microstructure–mechanical property relationships. Cellulose. vol. 17, pág. 661-669. 2010.

RINCÓN, J., OCAMPO, J. y BOADA, L. Estudio del desempeño de membranas de PVOH entrecruzadas con aldehído para la separación de mezclas agua-isopropanol. Tesis para la obtención del título de Ingeniero Químico. Departamento de Ingeniería Química. Bogotá, Universidad Nacional de Colombia. 2004.

ROSS, P., MAYER, R. y BENZIMAN, M. Cellulose Biosynthesis and Funtion in Bacteria. Microbiological Reviews vol. 55, pág. 35-58. 1991.

SAIBUATONG, O. y PHISALAPHONG, M. Novo aloe vera-bacterial cellulose composite film from biosynthesis. Carbohydrate Polymers. vol. 79(2), pág. 455-460. 2010.

SANCHAVANAKIT, N., SANGRUNGRAUNGROJ, W., y col. Growth of human Keratinocytes and fibroblasts on Bacterial Cellulose film. Biotechnology Progress. vol. 22, pág. 1194-1199. 2006.

SAXENA, I. y BROWN JR, M. Cellulose synthases and related enzymes. Current Opinion in Plant Biology vol. 3, pág. 523–531. 2000.

SCHAETZEL, P., FAVRE, E., y col. Mass-transfer through ion exchange membranes: comparison between the diffusion and the diffusion-convection Stefan-Maxwell equations. Electrochimica Acta. vol. 42(16), pág. 2475-2483. 1997.

SCHAETZEL, P., BENDJAMA, Z., y col. Ideal and non-ideal diffusion through polymers. Application to pervaporation. Journal of Membrane Science. vol. 191, pág. 95-102. 2001a.

SCHAETZEL, P., VAUCLAIR, C., y col. The solution–diffusion model: Order of magnitude calculation of coupling between the fluxes in pervaporation. Journal of Membrane Science. vol. 191, pág. 103-108. 2001b.

SCHAETZEL, P., VAUCLAIR, C., y col. A simplified solution–diffusion theory in pervaporation: the total solvent volume fraction model. Journal of Membrane Science. vol. 244(117-127). 2004.

SCHRAMM, M. y HESTRIN, S. Factors affecting Production of Cellulose at the Air/Liquid Interface of a Culture of Acetobacter xylinum. Journal of General Microbiology. vol. 11, pág. 123-129. 1954.

SCHRAMM, M., GROMET, Z. y HESTRIN, S. Synthesis of Cellulose by Acetobacter xylinum 3. Substrates and Inhibitors. Biochemical Journal. vol. 67(4), pág. 669-679. 1957.

SCHUMANN, D., WIPPERMANN, J., y col. Artificial vascular implants from bacterial cellulose: preliminary results of small arterial substitutes. Cellulose. vol., pág. ONLINE FIRST. 2008.

SERAFICA, G., MORMINO, R. y BUNGAY, H. Inclusion of Solid Particles in Bacterial Cellulose. Applied Microbiol Biotechnology vol. 58, pág. 756-760. 2002.

SHEN, W., CHEN, S., et al. Adsorption of Cu(II) and Pb(II) onto diethylenetriamine-bacterial cellulose. Carbohydrate Polymers. vol. 75(1), pág. 110-114. 2009.

SHIBAZAKI, H., KUGA, S., y col. Bacterial Cellulose as a Separation Medium. Journal of applied Polymer Science. vol. 50, pág. 965-969. 1993.

SHIBAZAKI, H., KUGA, S. y OKANO, T. Native Cellulose II production by *Acetobacter xylinum* under physical constraints. Cellulose. vol. 5, pág. 165-173. 1998.

SHIRK, H. y GREATHOUSE, A. Infrared Spectra of Bacterial Cellulose. Analytical Chemistry. vol. 24(11), pág. 1774-1775. 1952.

SOKOLNICKI, A., FISHER, R., y col. Permeability of bacterial cellulose membranes. Journal of Membrane Science vol. 272, pág. 15–27. 2006.

SON, H., HEO, M., y col. Optimization of Fermentation Conditions for the Production of Bacterial Cellulose by a Newly Isolated Acetobacter spA9 in Shaking Cultures. Biotechnology and Applied Biochemistry. vol. 33, pág. 1-5. 2001.

STERNBERG, L., DENIRO, M. y SAVIDGE, R. Oxygen Isotope Exchange Between Metabolites and Water During Biochemical Reactions Leading to Cellulose Synthesis. Plant Physiology. vol. 82, pág. 423-427. 1986.

STOICA-GUZUN, A., STROESCU, M., y col. Effect of electron beam irradiation on bacterial cellulose membranes used as transdermal drug delivery systems. Nuclear Instruments and Methods in Physics Research Section B: Beam Interactions with Materials and Atoms. vol. 265(1), pág. 434-438. 2007.

STRATHMANN, H. Membrane Separation Processes: Current Relevance and Future Opportunities. AIChE Journal. vol. 47(5), pág. 1077-1087. 2001.

STRATHMANN, H., GIORNO, L. y DRIOLI, E. An Introduction to Membrane Science and Technology. Rome, Institute of Membrane Technology CNR ITM. 2006.

STUART, B. Infrared spectroscopy: fundamentals and applications, John Wiley & Sons, Ltd. 2004.

SUN, D., YANG, J., y col. Novel Pd-Cu/bacterial cellulose nanofibers: Preparation and excellent performance in catalytic denitrification. Applied Surface Science. vol. 256(7), pág. 2241-2244. 2010.

SUÑOL, J., SAURINA, J., y col. Comparision of the Thermal Behavior of Three Cellullose Fibers Mercerized or Submitted to Solar Degradation. Journal of Thermal Analysis and Calorimetry. vol. 72, pág. 753-758. 2003.

SURMA-ŚLUSARSKA, B., PRESLER, S. y DANIELEWICZ, D. Characteristics of Bacterial Cellulose Obtained from Acetobacter Xylinum Culture for Application in Papermaking. FIBRES & TEXTILES in Eastern Europe vol. 16(4), pág. 108-111. 2008.

SVENSSON, A., NICKLASSON, E., y col. Bacterial cellulose as a potential scaffold for tissue engineering of cartilage. Biomaterials. vol. 26, pág. 419-431. 2005.

TAHARA, N., TONOUCHI, N., y col. Purification and Characterization of Exo-1,4-b-Glucosidase from Acetobacter xylinum BPR2001. Journal of Fermentation and Bioengineering vol. 85(6), pág. 589-594. 1998.

TAKE, H., YAMANAKA, S., y col. Anode performance of pyrolyzed bacterial cellulose in secondary lithium-ion batteries and the effect of added metal phthalocyanines. Japanese Journal of Applied Physics, Part 1. vol. 41(5A), pág. 3137-3139. 2002.

TAO, J. Effects of Molecular Weigth and Solution Concentration onelectrospinning of PVA. Materials Science and Engineering, Worcester Polytechnic Institute. 2003.

TAYLOR, R. y KRISHNA, R. Multicomponent Mass Transfer., John Wiley & Sons, Inc. 1993.

THOMPSON, D. y HAMILTON, M. Production of Bacterial Cellulose from Alternate Feedstocks. Applied Biochemistry and Biotechnology. vol. 91-93, pág. 503-513. 2001.

TIONGSON, J., BUGANTE, E. y DEL ROSARIO, E. Development of ultrafiltration membranes from bacterial cellulose (nata de coco) for the separation of mango volatile organic compounds. Philippine Agricultural Scientist. vol. 85(3), pág. 256-265. 2002.

TOMÉ, L., BRANDÃO, L., y col. Preparation and Characterization of Bacterial Cellulose Membranes with Tailored Surface and Barrier Properties. Cellulose. vol. 17, pág. 1203-1211. 2010.

TONOUCHI, N., HORINOUCHI, S., y col. Increased Cellulose Production from Sucrose by *Acetobacter* after introducing the sucrose phosphorylase gene. Bioscience, Biotechnology and Biochemistry. vol. 62(5), pág. 833-836. 1998a.

TONOUCHI, N., YANASE, H., y col. Increased Cellulose Production from Sucrose with Reduced Levan Accumulation by an Acetobacter Strain Harboring a Recombinant Plasmid. Bioscience, Biotechnology and Biochemistry. vol. 62(5), pág. 833-836. 1998b.

UHLIN, K., ATALLA, R. y THOMPSON, N. Influence of hemicelluloses on the aggregation patterns of bacterial cellulose. Cellulose vol. 2, pág. 129-144. 1995.

URAGAMI, T., SUGITANI,Y., SUGIHARA, M. Studies on Syntheses and Permeabilities of Special Polymer Membranes: 33. Permeation Behavior of Aqueous Alcohol Solution through Cellulose Membranes. Polymer. vol. 23(2), pág. 192-196. 1982.

VANDAMME, E., DE BAETS, S., y col. Improved production of bacterial cellulose and its application potential. Polymer Degradation and Stability vol. 59, pág. 93-99. 1998.

VEGA GARCÍA, M. y BONTOUX, L. "Food applications of new polysaccharides technology." www.jrc.es/iptsreport/vol20/english/FOOIE206.htm. 2001.

WADA, K. Modelagem e Simulacao de Separacao da Mistura Etanol-Agua por Pervaporacao. Tesis para La obtención de grado de doctor en Ingeniería. Programa de Pos-Graduacao de Engenharia, Universidade Federal do Rio de Janeiro. 1995

WADA, M., OKANO, T. y SUGIYAMA, J. Allomorphs of native crystalline cellulose I evaluated by two equatorial d-spacings. Journal of Wood Science. vol. 47, pág. 124-128. 2001.

WAN, Y., HUANG, Y., y col. Biomimetic synthesis of hydroxyapatite/bacterial cellulose nanocomposites for biomedical applications. Materials Science and Engineering: C. vol. 27(4), pág. 855-864. 2007.

WANG, Z., JIA, Y., y col. Research on characterization and biocompatibility of nano-bacterial cellulose membrane. Journal of Chinese Universities. vol. 30(8), pág. 1553-1558. 2009.

WANG, J., GAO, C., y col. Preparation and in vitro characterization of BC/PVA hydrogel composite for its potential use as artificial cornea biomaterial. Materials Science and Engineering C. vol. 30(1), pág. 214-218. 2010.

WANICHAPICHART, P., KAEWNOPPARAT, S., y col. Characterization of cellulose membranes produced by Acetobacter xyllinum. Songklanakarin Journal of Science and Technology. vol. 24 pág. 855-862. 2002.

WATANABE, K., ETO, Y., y col. A New Bacterial Cellulose Substrate for Mammalian Cell Culture. Cytotechnology. vol. 13, pág. 107-114. 1993.

WATANABE, K. y YAMANAKA, S. Effects of Oxygen Tension in the Gaseous Phase on Production and Physical Properties of Bacterial Cellulose Formed Under Static Culture Conditions. Bioscience, Biotechnology and Biochemistry. vol. 59(1), pág. 65-68. 1995.

WATANABE, K., TABUCHI, M., y col. Structural features and properties of bacterial cellulose produced in agitated culture. Cellulose. vol. 5, pág. 187-200. 1998.

WIJMANS, J. y BAKER, R. The Solution- Diffusion Model: A Review. Journal of Membrane Science. vol. 107, pág. 1-21. 1995.

WU, S. y LIA, Y. Application of bacterial cellulose pellets in enzyme immobilization. Journal of Molecular Catalysis B: Enzymatic. vol. 54, pág. 103-108. 2008.

YAMAMOTO, H. y HORII, F. In Situ crystallization of bacterial cellulose I. Influences of polymeric additives, stirring and temperature on the formation celluloses I_{α} and I_{β} as revealed by cross polarization/magic angle spinning (CP/MAS) 13C NMR spectroscopy. Cellulose. vol. 1, pág. 57-66. 1994.

YAMAMOTO, H., HORII, F. y HIRAI, A. In Situ crystallization of bacterial cellulose II. Influences of polymeric additives on the formation of celluloses Ia and Ib at the early stage incubation. Cellulose. vol. 3, pág. 229-242. 1996.

YAMANAKA, S., WATANABE, K. y KITAMURA, N. The structure and mechanical properties of sheets prepared from bacterial cellulose. Journal of Materials Science. vol. 24, pág. 3141-3145. 1989.

YANG, Y., PARK, S., y col. Cellulose Production by Acetobacter xylinum BRC5 under Agitated Condition. Journal of Fermentation and Bioengineering. vol. 85(3), pág. 312-317. 1998.

YANG, J., SUN, D., y col. In situ deposition of platinum nanoparticles on bacterial cellulose membranes and evaluation of PEM fuel cell performance. Electrochimica Acta. vol. 54(26), pág. 6300-6305. 2009.

YASUDA, K., GONG, J., y col. Biomechanical properties of high-toughness double network hydrogels. Biomaterials. vol. 26, pág. 4468–4475. 2005.

YOSHINAGA, F., TONOUCHI, N. y WATANABE, K. Research Progress in production of Bacterial Cellulose by Aeration and Agitation Culture and Its application as a New Industrial Material. Bioscience, Biotechnology, Biochemistry. vol. 61, pág. 219-224. 1997.

XYLOS Corp. http://www.xyloscorp.com/content/technology/core.php, 2011.

ZAAR, K. Visualization of Pores (Export Sites) Correlated with Cellulose Production in the Envelope of the Gram-negative Bacterium *Acetobacter xylinum*. Journal of Cell Biology. vol. 80, pág. 773-777. 1979.

ZABOROWSKA, M., BODIN, A., y col. Microporous bacterial cellulose as a potential scaffold for bone regeneration. Acta Biomaterialia. vol. Article in Press. 2010.

ZAHEDMANESH, H., GATENHOLM, P. y LALLY, C. Bacterial cellulose: A potential vascular graft and tissue engineering scaffold. Proceedings of the ASME Summer Bioengineering Conference 2009, SBC2009, (PART A). vol., pág. 519-520. 2009.

ZHANG, S., XIONG, G., y col. Characterisation of hydroxyapatite/bacterial cellulose Nanocomposites. Polymers and Polymer Composites. vol. 17(6), pág. 353-358. 2009.

ZHENG, Q., XI, T., y col. Cytocompatibility of nano-hydroxyapatite/bacterial cellulose nanocomposites and its residues. Journal of Clinical Rehabilitative Tissue Engineering Research. vol. 14(3), pág. 405-409. 2010.

ZHOU, L., SUN, D., y col. Effect of addition of sodium alginate on bacterial cellulose production by Acetobacter xylinum. Journal of Industrial Microbiology and Biotechnology. vol. 34, pág. 483-489. 2007.

ZIMMERMANN, K., LEBLANC, J., y col. Biomimetic design of a bacterial cellulose/hydroxyapatite nanocomposite for bone healing applications. Materials Science and Engineering C. vol. Article in Press. 2009.

ZUO, K., CHENG, H., y col. A hybrid model combining hydrodynamic and biological effects for production of bacterial cellulose with a pilot scale airlift reactor. Biochemical Engineering Journal vol. 29, pág. 81–90. 2006.